Design of environmentally friendly neonicotinoid insecticides with bioconcentration tuning and Bi-directional selective toxic effects

Yuanyuan Zhao [a, b], Yu Li [a, b, *]

[a] College of Environmental Science and Engineering, North China Electric Power University, Beijing, 102206, China
[b] The State Key Laboratory of Regional Optimisation of Energy System, North China Electric Power University, Beijing, 102206, China

ABSTRACT

A 3D-QSAR model was established with CoMSIA to characterize neonicotinoid insecticides. LgBCF values were used as the dependent variable and the molecular structures of 30 compounds were used as the independent variable. This model was used to design neonicotinoid insecticides with reduced bio-concentration. The contour maps from the 3D-QSAR model were used to evaluate substituted sites and different substituents that significantly affected the bioconcentration of neonicotinoid insecticides. The CoMSIA model showed that neonicotinoid insecticide bioconcentration was strongly affected by steric, electrostatic, hydrophobic and hydrogen bond acceptor fields. Using compound 20 as a template, 105 new substituted derivatives with lower bioconcentrations (reduced by 21.34—77.21%) were designed. The toxicities of these derivatives were evaluated, which showed that 100 of the derivatives retained the original toxicity (increased by 0.10—5.67%). Next, a 2D-QSAR model showed that the decreased bio-concentration of the new neonicotinoid insecticides was mainly caused by the total energy and dipole moment. Homology modeling was used to obtain the genetic recombination AChR in sucking-type pests (i.e. aphid, leafhopper, thrips, and *Bemisia tabaci*) and bees (i.e. Apis mellifera ligustica and Apis cerana). The neonicotinoid insecticides before and after modification were docked with AChRs to complete the screening of derivatives with bi-directional selective toxic effects. LibDock scores showed that Derivative-5, Derivative-18, Derivative-31, and Derivative-65 had bi-directional selective effects on pests and bees. The effects of the Derivative-18 were the most significant, with toxicity increasing by 14.66% in pests and decreasing by 19.42% in bees. We determined via analysis of amino acid residues that Derivative-18 had more hydrophobic amino acids interacting with pest AChRs, and the mode of action was predominantly hydrogen bonding. Conversely, Derivative-18 had fewer hydrophobic amino acids interacting with bee AChRs, and the mode of action there was more reliant on van der Waals forces with weak binding power.

© 2019 Elsevier Ltd. All rights reserved.

1. Introduction

In the past fifty years, pesticides—i.e. chemical agents used to control pests—have been constantly enriched and improved. These improved agents include organophosphorus pesticides, which are used in forestry and agriculture to control a variety of pests, including livestock parasites. However, many of these agents are highly toxic to both humans and livestock, which can lead to lung paralysis and death. Pyrethroid pesticides kill many insects on contact, and are highly efficient and have low toxicity. In addition, these pesticides are capable of fast knockdown, and are safe for both humans and animals, showing little residue. However, due to the short residue period, they also decompose readily (Tush and Anstead, 1997).

Neonicotinoid insecticides are newer pesticides based on the structure of nicotine. They are used extensively in agriculture because of their high efficiency, high selectivity, high persistence, and low toxicity to mammals (European Food Safety Authority, 2013). However, despite the fact that these insecticides can effectively prevent and control harmful insects, they are also harmful to pollinators (Goulson et al., 2015). Because pollinators—especially bees—have considerable economic value, exposure to excess pesticide in the air or on the surface of the plant during the

* Corresponding author. North China Electric Power University, No.2, Beinong Road, Beijing, 102206, China.
E-mail addresses: zyy950210@outlook.com (Y. Zhao), liyuxx8@hotmail.com (Y. Li).

collection of nectar and pollen is a considerable danger. This exposure affects bee behavior, nutrient metabolism, and immune function (Belzunces et al., 2012). Moreover, other pollinators also face similar threats from neonicotinoid insecticides.

In 2010, Mullin et al. gathered crop samples from 23 states and analyzed bee and hive matrices for pesticide residues using LC–MS/MS and GC–MS. They found high levels of pesticide residues in beeswax and pollen, and lower levels in adult bees and larvae (Mullin et al., 2010). In 2011, Tapparo et al. used ultra-high perfor-mance liquid chromatography–diode array detection to analyse guttation drops of corn plants from commercial seeds coated with thiamethoxam, clothianidin, and imidacloprid (Tapparo et al., 2011). The concentration of imidacloprid in the drops was found to be as high as 346 mg/L, while the concentrations of thiame-thoxam and clothianidin reached 146 mg/L and 102 mg/L, respec-tively. In 2012, Pohorecka used QuEChERS extraction and LC–MS/MS to analyse five neonicotinoid insecticides (imidacloprid, clo-thianidin, thiamethoxam, acetamiprid, and thiacloprid) using a multi-residue method. This protocol was highly specific and very sensitive, with a detection limit of 10^{-4}~10^{-2} mg/L (Williamson et al., 2014). In the same year, Dively et al. sprayed neonicotinoid insecticides directly onto pumpkin leaves. Subsequently, dinote-furan and thiamethoxam were detected in pollen at concentrations of 0.036–0.147 mg/L and of 0.061–0.127 mg/L, respectively (Dively and Kamel, 2012).

High levels of pesticide residue in crops and the environment adversely affect the health of humans, livestock, and especially pollinators (Cai et al., 2012). Henry et al. established a bee colony simulation model to monitor the foraging behavior of bees over a 1-month period (Henry et al., 2012). The normal foraging time of the bees was 300s, but after eating sublethal doses of imidacloprid and thiamethoxam, they showed a poorer ability to identify foraging sites, a longer homing time, and a lower number of daily round trips. In addition, Yang et al. recorded the capped-brood, pupation, and eclosion rates of honeybee larvae after treating them directly in the hive with different doses of imidacloprid (Yang et al., 2012). They found that brood-capped rate decreased significantly when the dose increased from 24 to 8×10^{-3} mg. Although there was no significant effect of imidacloprid (4×10^{-7} mg) on the brood-capped, pupation, and eclosion rates, the olfactory associative behavior of the adult bees was found to be impaired. In similar experiments, Tan et al. found that after consuming a dose of 34 mg/L imidacloprid syrup, the number of *Apis cerana* field bees was reduced by 23% and the collection ability of those that survived was reduced by 46% (Tan et al., 2014). Similar to use spectrophotometry to adsorb cationic dyes (Dil et al., 2016, 2017, 2018; Dil et al., 2017a,b).

In this study, we designed 105 derivatives from compound 20, and their toxicities were evaluated to ensure insecticidal efficacy (Chen et al., 2016). Finally, the bi-directional selective toxic effects of Derivative-18 were screened by homology modeling and mo-lecular docking. This theoretical method can be used in the future to study neonicotinoid insecticide bioconcentration, selective toxic effects, and resistance.

2. Materials and methods

2.1. Data

3D-QSAR models were analyzed using SYBYL molecular modeling software (Gu et al., 2016). Experimental data for the neonicotinoid insecticides analyzed were determined using EPI Suite. For convenience, lgBCF values were included in the experi-mental data. To ensure structural diversity of compounds and a universal distribution, 23 compounds were included in a training

set and 8 compounds were included in a test set (Adnane et al., 2017). Compound 20 was included in both sets.

2.2. 3D-QSAR models for neonicotinoid insecticide bioconcentration

2.2.1. Molecular structure modeling and alignment of neonicotinoid insecticides

The molecular structures of all compounds were drawn directly in SYBYL-X and were then optimized to find their most stable conformations. Compound optimization was performed by considering the Tripos force field and used Gasteiger-Hückel charges (Reihaneh and Jahan, 2013). Powell's method was used with a maximum of 10,000 optimizations and an energy conver-gence gradient value of 0.005 kJ/mol; all other parameters were set to default values (Wang et al., 2017a,b).

All molecules had common characteristic elements found in the labeled region (shown in Fig. 1). We used Compound 20, which had the largest lgBCF value, as the target to align the rest of the mole-cules. All compounds could be well aligned.

2.2.2. Model of neonicotinoid insecticides

Using the QSAR module, CoMSIA was selected as the analysis method, and we calculated the electrostatic field, steric field, hy-drophobic fields, and hydrogen-bond donor and acceptor fields of all compounds. The dielectric constant was related to distance, the threshold was 125.4 kJ/mol, and all other parameters were set to their default values (Gu et al., 2017). The 30 lgBCF values of the neonicotinoid insecticides were entered into the training table, and the parameters of the model were calculated automatically by Autofill using SYBYL-X. Partial least-squares regression analysis was applied to establish the relationships between the structures and biological activities of the target compounds. First, we used the leave-one-out method to cross-validate the training set compounds and determined the values of q^2 and n. Next, non-cross-validation analysis was conducted to obtain the r^2, the F, and the SEE values. The results of the CoMSIA method were largely unaffected by the rules of compound matching, and this may explain the structure–activity relationship of a compound.

2.3. Homology modeling for acetylcholine receptors

A homology modeling algorithm was used to predict synthetic receptor protein structures based on the known structures of pro-tein. The amino acid sequences of the AChRs (GI: 347948662; PDB: 3SQ9) were obtained from the NCBI. The amino acid sequences of the AChRs and the target protein were submitted to the SWISS-MODEL automated protein modeling server (GlaxoSmithKline, Geneva, Switzerland) and the protein structure of the AChRs was obtained by homology modeling. For the target protein, we eval-uated the structural rationality of the model using the Ramachan-dran conformation map in PROCHECK. Generally, the sum of base percentages in the core area, allowable area, and maximum allowable area was greater than 95%, which met the quality re-quirements of the model.
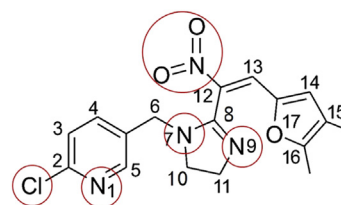

Fig. 1. The structure of Compound 20 and the align of common framework.

2.4. Docking method for neonicotinoid insecticides before and after modification with AChRs

Next, we conducted computational simulations using Discovery Studio 4.0. For each compound in the Tripos force field, the molecular program Minimize was used to optimize the energy according to their Gasteiger-Huckel charge (Wang et al., 2017a,b; Gu et al., 2017). Using Powell's method, the energy convergence was limited to 0.005 kJ/mol and the maximum number of optimizations was 10,000. Finally, using Dock Ligands module in Discovery Studio 4.0, we determined the receptor binding cavity of all AChRs and ligand molecules were incorporated into the formed protein binding cavity for flexible docking (Arnold et al., 2006).

3. Results and analysis

3.1. Evaluation and analysis of the CoMSIA model for neonicotinoid insecticide bioconcentration

In the CoMSIA model, the contribution rates of the steric, electrostatic, hydrophobic, hydrogen-bond donor and acceptor fields were 17.30%, 32.50%, 6.10%, 13.70%, and 30.40%, respectively. These results showed both that all fields affected the lgBCF values of neonicotinoid insecticides, and that the electrostatic interaction field had the largest contribution rate.

Our model gave the following validation data: $n = 10$, $q^2 = 0.653$ (>0.5), and the model should be considered reliable, $r^2 = 0.992$ (>0.9), and SEE = 0.074. These results suggested that this model had an adequate predictive capability. Moreover, the stability parameters, the Q^2 value, and the dq^2/dr^2yy ratio also indicated that the model had good stability (Table 1) (Salahinejad and Ghasemi, 2013).

3.2. Prediction of neonicotinoid insecticide LgBCF based on CoMSIA model

The activity of a test set was predicted by the model to test its accuracy. The SEP value of our model was 0.651, and the Q^2_{ext} was 0.028. These results verified the predictive power of the 3D-QSAR model, could therefore reliably be used to predict the lgBCF values for the 30 neonicotinoid insecticides (Table 2).

A linear analysis of the experimental and predicted values of the lgBCF values in the CoMSIA model was conducted. The relevant equation for the CoMSIA model was:

$$y = 0.5417x + 0.8585 \ (r = 0.5024) \tag{1}$$

This result showed that the predicted lgBCF showed good linear dependence ($n = 30$, $p = 0.01$, $r_{min} = 0.5024 > r$: 0.4487). The model had significant predictive value and could therefore be used to predict the lgBCF values of the neonicotinoid derivatives (Wang et al., 2017c).

3.3. Design of neonicotinoid derivatives based on 3D-QSAR model

3.3.1. Determination of substitution sites and substituent groups based on contour maps

The contour maps of the CoMSIA (Fig. 2) model were constructed with the target compound. The different coloured contour map regions around the target compound show the respective influences of the electrostatic, steric, hydrophobic, and hydrogen-bond acceptor and donor fields on the lgBCF values of each of the neonicotinoid insecticides. The standard deviation and the coefficient are also shown in the contour maps with a favored threshold of 80% and a disfavored threshold of 20%. With respect to the electrostatic field, blue contours show that positive charges increase the activity of the molecules, while red contours show that negative charges increase the activity of the molecules. In the steric field, green contours show that bulky groups increase the activity of the molecules, and yellow contours show that bulky groups reduce the activity of the molecules. In the hydrophobic and hydrophilic fields, favorable contributions are shown in yellow and white contours, respectively (see Fig. 3).

The CoMSIA steric contour map showed yellow contours around the 4-, 8-, 10-, and 11- positions of the neonicotinoid insecticides, which showed that the introduction of bulky groups to these positions could reduce the lgBCF values, and thereby decrease their bioconcentration. Similarly, the electrostatic contour map showed red contours around the 4-, 9-, and 10- positions of the neonicotinoid insecticides, meaning that the introduction of electropositive groups could decrease the lgBCF values. With respect to the hydrophobic contour map, white contours around the 4-, 10-, and 15- positions of the neonicotinoid insecticides showed that the introduction of hydrophobic groups at these positions could reduce the lgBCF values. The hydrogen-bond acceptor contour maps showed purple regions around the 4- and 10- positions of the neonicotinoid insecticides, which suggests that hydrogen donor groups at these positions would also decrease the lgBCF values. In contrast, the contours in the hydrogen-bond donor contour map did not impact the substituents.

In summary, the CoMSIA model contour maps showed yellow, red, white, and purple contours around the 4- and 10- positions of the target compound, yellow contours around the 8- and 11- positions, red contours around the 9- position, and white contours around the 15- position. Thus, the 4- and 10- positions were affected by the electrostatic, steric, hydrophobic, and hydrogen-bond acceptor fields, implying that the introduction of bulky, electropositive, hydrophobic, or hydrogen donor groups at the 4- and 10- positions may reduce the lgBCF values. Similarly, introduction of bulky groups at the 8- and 11- positions, electropositive groups at the 9- position, and hydrophobic groups at the 15- position could also reduce the lgBCF values. Based on this analysis, substitution at the 4- and 10- positions of the target compound was performed with ten groups ($-OH$, $-COOH$, $-Br$, $-I$, $-CHO$, $-SO_2$, $-SO_3H$, $-SH$, $-CO$, and $-NO_2$) to generate 105 derivatives.

3.4. Evaluation of the bioconcentration and toxicity characteristics and the mechanism analysis of compound 20 both before and after modification

3.4.1. Evaluation of bioconcentration and toxicity of compound 20 before and after modification
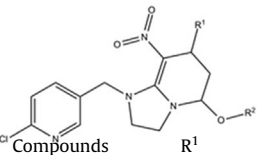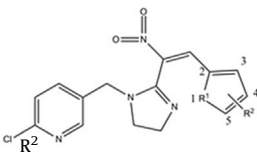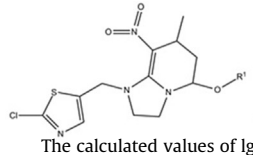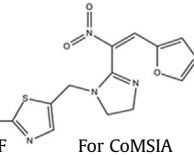
Thus far, in this study we had predicted the lgBCF and pLC_{50} values of the 105 derivatives. Our bioconcentration results showed that the lgBCF values of all derivatives were lower than that of the target compound. With the exceptions of Derivative-7, Derivative-

Table 1
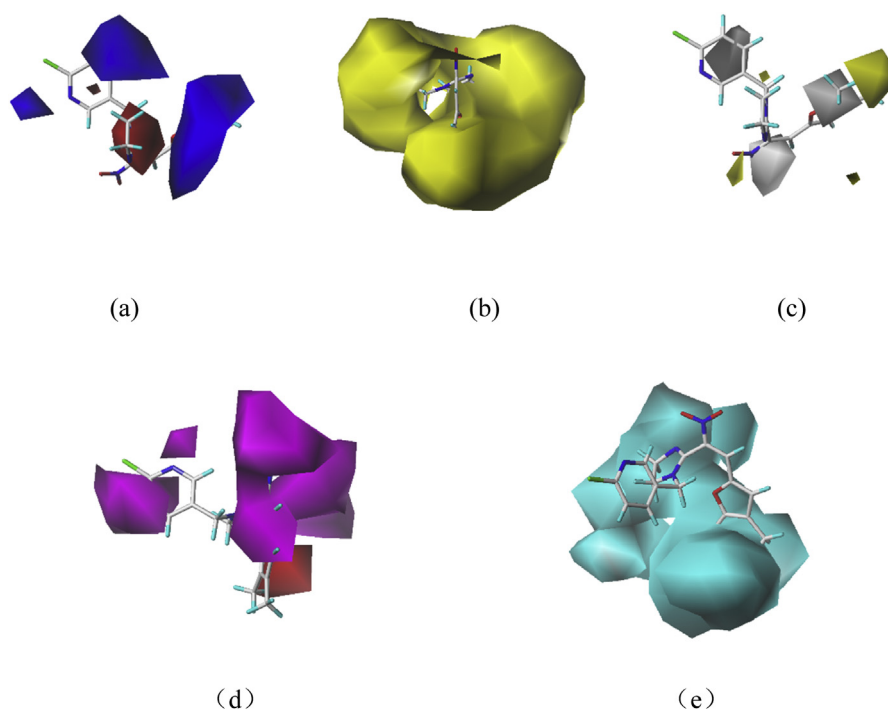Evaluation parameters of CoMSIA model.

Model	q^2	n	SEE	r^2	F	SEP	Q^2	SDEP	dq^2/dr^2yy
CoMSIA	0.653	10	0.074	0.992	152.354	0.651	0.443	0.619	1.771

Table 2
Experimental and calculated lgBCF values of neonicotinoid derivatives.

Compounds	R^1	R^2	The calculated values of lgBCF	The predicted values of lgBCF	Relative error (%)
	1-16	17-27	28-29	For CoMSIA 30	
1	$-CH_3$	$-H$	0.50	0.484	−3.20
2	$-CH_3$	$-CH_3$	0.36	0.391	8.61
3	$-CH_3$	C_2H_5	0.69	0.696	0.87
4	CH_3	n-Propyl	0.50	0.492	−1.60
5	CH_3	C_2H_4Cl	0.86	0.844	−1.86
6	C_2H_5	H	0.50	0.478	−4.40
7	CH_3	iso- Propyl	0.50	0.492	−1.60
8	C_2H_5	C_2H_5	1.01	1.041	3.07
9	C_2H_5	n-Propyl	0.11	0.112	1.82
10	C_2H_5	iso- Propyl	0.50	0.475	−5.00
11	H	H	0.50	0.522	4.40
12	H	CH_3	0.50	0.512	2.40
13	H	C_2H_5	0.41	0.430	4.88
14	H	n-Propyl	0.50	0.497	−0.60
15	H	Benzyl	1.71	1.785	4.39
16	H	2-Chloro-5-Methyl-Pyridinyl	1.42	1.407	−0.92
17	O	−	1.35	1.450	7.41
18	O	$5-CH_3$	1.71	1.768	3.39
19	O	$5-C_2H_5$	2.03	1.968	−3.05
20	O	$4,5-(CH_3)_2$	2.07	1.960	−5.31
21	O	$5-CH_2OH$	0.49	0.508	3.67
22	O	5-Br	1.94	1.762	−9.18
23	O	$5-NO_2$	1.23	1.233	0.24
24	S	−	1.65	1.746	5.82
25	S	$5-CH_3$	2.01	2.000	−0.50
26	NH	−	1.03	0.977	−5.15
27	C	5-O	1.35	1.235	−8.52
28	H	−	0.50	0.511	2.20
29	C	−	0.50	0.518	3.60
30	−	−	0.57	0.565	−0.88

* representing the target database in this manuscript.

Fig. 2. Contour maps for CoMSIA model electrostatic field (a), steric field (b), hydrophobic field (c), and hydrogen bond acceptor (d) and donor fields (e).
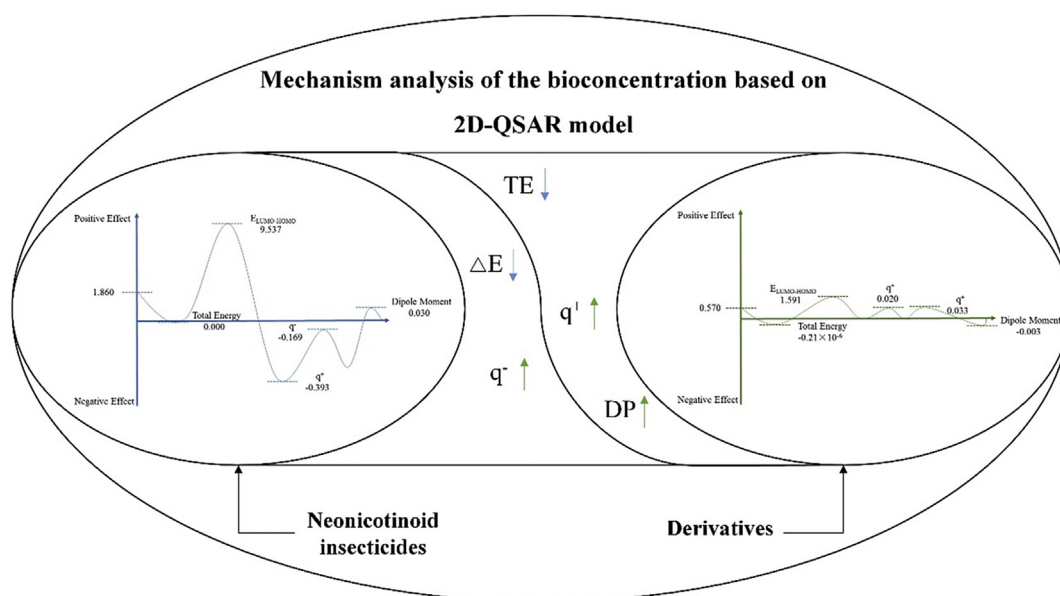
Fig. 3. Mechanism analysis of bioconcentration of neonicotinoid insecticides and derivatives.

14, Derivative-39, Derivative-66 and Derivative-91, the lgBCF values of the remaining derivatives were reduced by over 50%, which indicated that the derivatives had bioconcentrations that were significantly lower than the target compound.

Our toxicity results showed that the pLC$_{50}$ values of Derivative-21, Derivative-66, Derivative-67, Derivative-75 and Derivative-76 were slightly lower (i.e. showed a <2% difference) than the target compound, which indicated slightly reduced toxicity. Studies on these 5 derivatives were discontinued to ensure that the new pesticides were as effective as the target compound. The pLC50 values of the remaining 100 derivatives were not significantly different (i.e. increased by 0.10—5.67%) from the target compound, indicating that these derivatives were less toxic.

3.4.2. Mechanism analysis for compound 20 before and after modification through a 2D-QSAR model

Compound 20—both before and after modification—was selected for further QSAR modeling using multiple linear regression. The lgBCF values were used as the dependent variable, and the TE (eV), $\triangle E$ (eV), q^+ (e), q^- (e), and DP (Debyes) were used as independent variables. The equations relating the neonicotinoid insecticides and the 100 derivatives to their quantum chemical parameters are given below.

Molecular equation for the neonicotinoid insecticides:

$$lgBCF = 1.860 + 9.537\triangle E - 5.393q^+ - 0.169q^- + 0.030DP \quad (2)$$

Molecular equation for the 100 derivatives:

$$lgBCF = 0.570 - 0.21 \times 10^{-6}\,TE + 1.591\triangle E + 0.020q^+ + 0.033q^- - 0.003DP \quad (3)$$

The R value of the neonicotinoid insecticides and the 100 derivatives in the QSAR model were 0.729 ($n = 30$, $p = 0.05$, $r_{min} = 0.729 > r$: 0.3494) and 0.229 ($n = 100$, $p = 0.05$, $r_{min} = 0.229 > r$: 0.1946), respectively. From Eq. (2), the coefficients of $\triangle E$ and DP were positive, q^+ and q^- were negative, and the TE was zero. This indicated that $\triangle E$ and DP had positive effects, q^+ and q^- had negative effects, and the TE had no effect on the bioconcentration of the neonicotinoid insecticides. The coefficients of

q^+ and q^- of the 100 new putative neonicotinoid insecticides were positive in Eq. (3), which indicated that they had positive effects on pesticide bioconcentration. The TE and DP coefficients were negative, thus indicating that they had a negative effect on pesticide bioconcentration. The $\triangle E$ value showed no change compared with Eq. (2). By comparing the effects of various quantification parameters on pesticide bioconcentration, we found that the decreased bioconcentration of the new neonicotinoid insecticides was mainly caused by TE and DP. This provides a theoretical basis for future analyses of the mechanism(s) of bioconcentration of neonicotinoid insecticides and their derivatives (Tong et al., 2016).

3.5. Bi-directional selective toxic effects of new neonicotinoid insecticides with AChRs through homology modeling and molecular docking

3.5.1. Homology modeling for AChRs

Since neonicotinoid insecticides do not have selective toxic effects on sucking-type pests (aphid, leafhopper, thrips, and *Bemisia tabaci*—hereafter referred to as 'pests') and bees (i.e. Apis mellifera ligustica and Apis cerana; hereafter referred to as 'bees') we studied the bi-directional modification of the AChRs in both pests and bees to ensure that their toxic effects on pests were increased and their chronic sublethal effect on bees was reduced. Based on the contour maps shown above, hydrophobic amino acids appeared to increase pesticide toxicity, while hydrophilic amino acids did not. Therefore, the hydrophilic residues in the pest-linked AChR amino acid sequence were adjusted to hydrophobic amino acids, such as Asn to Ile (No. 92) and Ser to Phe (No. 95). However, for gene recombination of AChRs in bees, some hydrophobic residues were changed to hydrophilic residues, such as Ile to Arg (No. 94) and Pro to Lys (No. 97). The results were showed in Fig. 4, generating by the SWISS-MODEL automated protein modeling server.

According to the rational evaluation of the target protein structure, all amino acid residues of the two proteins were located in the permissible region, while the percentage of the base area (84.5%, 91.4%), permissible area (12.7%, 8.1%), and maximum allowed region (2.2%, 0.5%) equated to 99.4% and 100%, which exceeded the model quality requirement (95%).
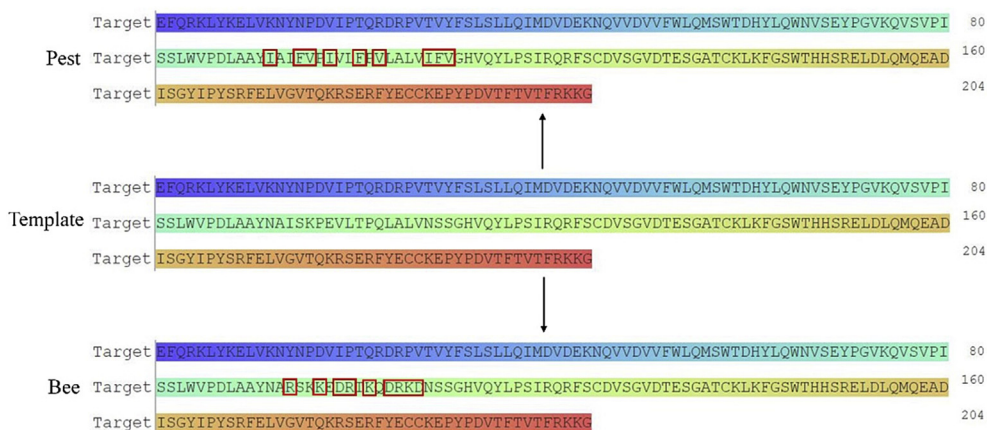
Fig. 4. Amino acid sequence after modification of AChRs in pests and bees.

3.5.2. Molecular docking analysis of compound 20 before and after modification with AChRs

Compound 20 before and after modification were docked with the AChRs (in pests and bees) using Discovery Studio software. The results showed that for the pests, the LibDock scores of compound 20 before and after modification with AChRs showed that 49 derivatives showed increased insecticidal effects compared with the target compound. The maximum increase was 35.10%, and the smallest increase was 2.84%, which indicated increased likelihood to bind to AChRs in pests, impede the transmission of cholinergic signals, control pest behavior, and cause paralysis and death. Thus, the lethal effects of pesticides on insect pests are predicted to be enhanced. In addition, the chronic sublethal effects of insecticides on bees were also examined. To do so, the target compound and 49 derivatives were docked with AChRs in bees to further screen for environmentally friendly new neonicotinoid insecticides. The LibDock scores of Derivatives-5, Derivatives-18, Derivatives-31, and Derivatives-65 were 4.83%, 19.42%, 2.80%, and 0.08% lower than that of the target compound, respectively. This indicated that the binding ability of AChRs was decreased, thus reducing the chronic sublethal effects of pesticide exposure to bees.

Taken together, our data suggest that Derivative-5, Derivative-18, Derivative-31, and Derivative-65 can provide decreased bioconcentration and increased toxicity. Ideally, the bi-directional selective toxic effects to the AChRs enhanced the lethal effect on pests and reduced the chronic sublethal effect on bees. The lethal effect to pests of Derivative-18 increased by 14.66%, and its lethal effect to bees decreased by 19.42%. Because of its efficacy, we investigated the toxicity mechanism of Derivative-18 further.

3.5.3. Mechanistic analysis of bi-directional selective toxic effects through amino acid residues

When Derivative-18 combined with AChRs, we found that amino acid residues within a certain distance of the AChR played a major role. These amino acids were deemed to be 'active residues'. In addition, hydrogen bonds were of major importance in defining the structure and function of compounds, including the binding of ligands to protein receptors. Therefore, this study mainly analyzed the properties of amino acid residues (Table 3) and the role played by hydrogen bonds.

Table 3 shows that the amino acids that interacted with Derivative-18 included both hydrophobic amino acids, (i.e. Tyr, Pro, Trp, Leu, Val, and Ile) and hydrophilic amino acids (i.e. Asp, Ser, His, Gln, and Thr). In pests, nine hydrophobic amino acids and seven hydrophilic amino acids were found to be involved in the binding of

Table 3
Properties of amino acid residues.

Residue	Hydrophobic value	The number of residues	
		Pest	Bee
Tyr	0.26	4	–
Pro	0.12	1	3
Asp	−1.05	1	3
Ser	−0.18	1	2
His	−0.40	1	1
Trp	0.81	1	1
Cys	0.29	2	–
Leu	1.06	3	1
Gln	−0.78	1	1
Thr	−0.05	1	–
Val	1.08	–	1
Ile	1.38	–	1

Derivative-18 to AChRs. However, in bees, the number of hydrophobic amino acids found to interact with Derivative-18 decreased to seven, but the number of hydrophilic amino acids remained the same. We found that the hydrophobic regions formed by hydrophobic amino acids played a significant role in hydrophobic interaction between AChRs and Derivative-18. When Derivative-18 entered into hydrophobic AChRs, the hydrophobic interaction force increased, and the affinity of the molecule and the AChRs in the pests was enhanced, resulting in a higher LibDock score. Conversely, when Derivative-18 entered less hydrophobic AChRs, the hydrophobic interaction force was lower, the molecular affinity between Derivative-18 and the bee AChR was weakened, and the LibDock score was lower.

The interactions between amino acids and Derivative-18 were mainly divided into two categories (Fig. 5). For pest AChRs, Tyr91, Tyr184, Trp145, Tyr191, Cys186, Cys187, Thr146, Ser144, His147, Pro192, and Asp193 (coded pink) used hydrogen bonding and electrostatic forces to stabilize receptor protein–ligand complexes. Only the interaction between Tyr91 and Thr146 and Derivative-18 specifically used hydrogen bonding. Moreover, Leu116, Leu104, Gln114, Tyr115, and Leu106 (coded green) used van der Waals forces to stabilize receptor protein–ligand complexes. In contrast, Ser77, Trp84, Pro16, Val85, His147, Asp17, Pro86, and Asp87 were coded pink for bee AChRs. In bees, only Val85 interacted via hydrogen bonding, both as donor and receptor, while Asp104, Ser81, Leu83, Gln103, Ile80, and Pro79 were coded green.

Taken together, our comparative analysis indicated that in pest AChRs, Derivative-18 interacted primarily with hydrophobic amino
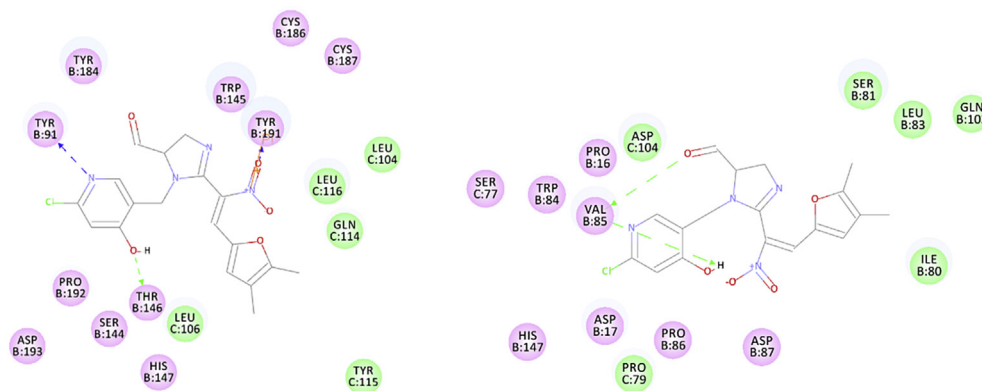
Fig. 5. Planar graph of key amino acids of AChRs binding with Derivatives-18.

acids, predominantly via hydrogen bonding. Conversely, in bee AChRs, the number of hydrophobic amino acids involved was fewer, and the mode of action was more reliant on van der Waals forces with weak binding power. Although some hydrogen bonding was apparent, the amino acids acted as both hydrogen bonding donors and acceptors. Thus, the binding capacity to the AChRs was somewhat weaker. An overview of this process is shown in Fig. 6.

3.6. Practical evaluation of new neonicotinoid insecticides

We further identified the practical characteristics of Derivative-5, Derivative-18, Derivative-31, and Derivative-65. Taking Compound 20 as an example, the ΔG in the reaction temperature of 300 K for four substitution reactions could be calculated using Eq. (4) to determine the possibility of a substitution reaction.

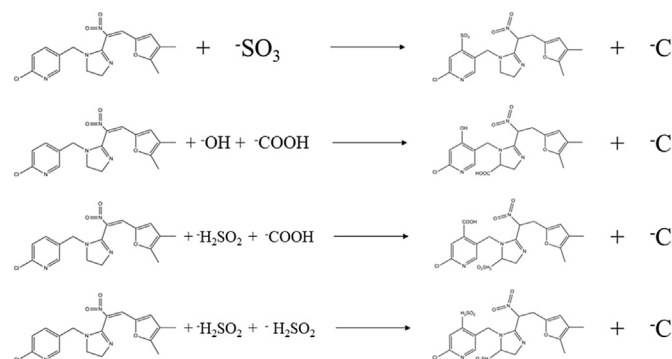$$\Delta G = \sum G(\text{product}) - \sum G(\text{reactant}) \tag{4}$$

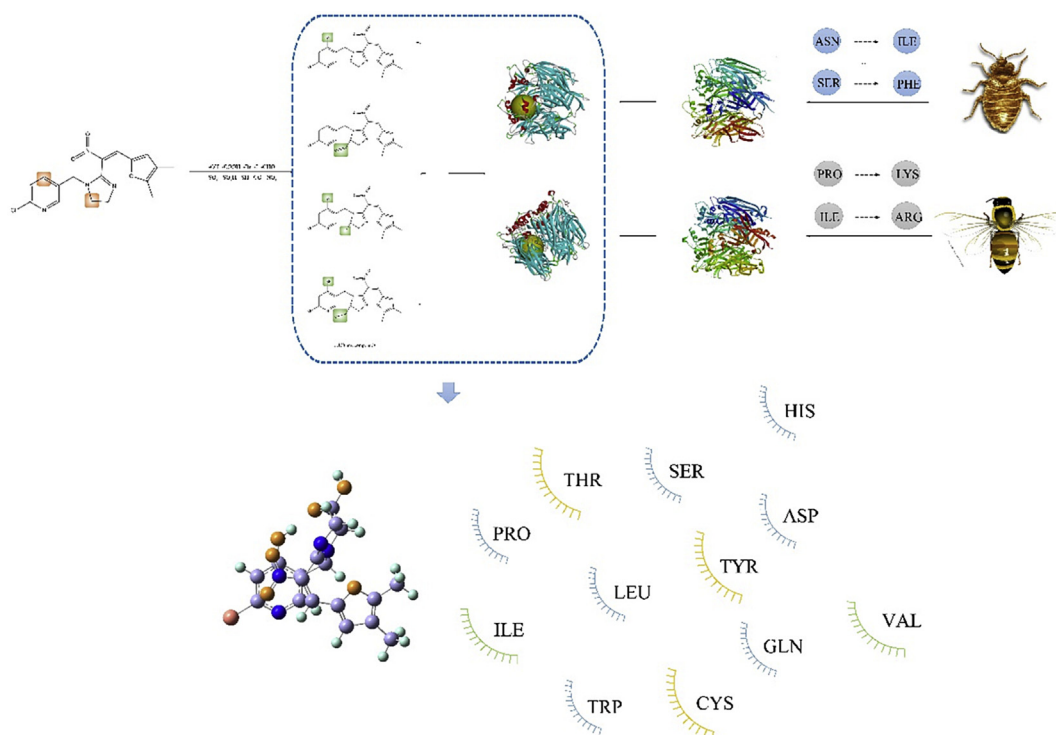**Fig. 7.** The substitution reaction paths of neonicotinoid insecticides.

Fig. 6. Mechanism of selective toxicity of derivatives to pests and bees.

Table 4
Calculations of the positive frequency for four neonicotinoid derivatives, Gibbs free energy, and energy barrier for four chemical reactions.

Compounds	Frequency/(cm^{-1})	Paths	ΔG/(a.u.)	ΔE/(a.u.)
Derivative-5	12.98	Path 5 (4-SO$_3$)	−0.0199	32.5332
Derivative-18	12.03	Path 18 (4-OH,10-COOH)	−0.2674	29.6412
Derivative-31	11.96	Path 31 (4-COOH,10-H$_2$SO$_2$)	−0.0374	18.0423
Derivative-65	13.61	Path 65 (4-H$_2$SO$_2$,10-H$_2$SO$_2$)	−0.0219	21.7242

In addition to analyzing the possibility of substitution reactions, we also compared their difficulty. In this paper, the TS and ΔE of the substitution reaction were calculated according to density functional theory. The transition state was verified by intrinsic co-ordinates, and only one imaginary frequency was needed to replace the reaction energy barrier (Eq. (5)). The results of the above calculation are shown in Table 4.

$$\Delta E = E(TS) - \sum E(\text{reactant}) \tag{5}$$

This data showed that the positive frequencies of the four neonicotinoid derivatives were all greater than 0. The positive frequencies represented the lowest energy in a particular dimension, indicating that all four neonicotinoid derivatives had stable structures and could therefore exist stably in the environment. Meanwhile, the ΔG values of the four neonicotinoid derivatives were less than 0, indicating that the substitution reaction could proceed spontaneously, and the inferred substitution reaction was reasonable. The rank order of the difficulty of substitution reaction was Derivative-5 > Derivative-18 > Derivative-65 > Derivative-31 (Hajipour et al., 2016).

4. Conclusions

In this study, 105 new neonicotinoid insecticides were designed to have a lower bioconcentration (which was reduced by 21.34% ~77.21% compared to the target molecule No. 20), and a toxicity that was not significantly lower than Compound 20 (lower by −1.41% ~5.67%). A mechanistic analysis of the decrease in bioconcentration between 30 neonicotinoid insecticides and 100 neonicotinoid derivatives using a 2D-QSAR model indicated that the reduction in bioconcentration of the modified derivatives was mainly caused by differences in the total energy and dipole moment. Finally, homology modeling and molecular docking methods showed that four of the new neonicotinoid insecticides had bi-directional selective toxic effects on pests and bees. Of these four, Derivative-18 showed an increase in its lethal effect on pests (i.e. an increase of 14.66%) and a decrease in its chronic sublethal effect on bees (i.e. a decrease of 19.42%). These results—as well as the accompanying method—provide a theoretical basis both for the further study of pest resistance to neonicotinoid insecticides as well as the modification of neonicotinoid derivatives to have fewer harmful environmental effects. We believe that these findings may therefore accelerate the development of new pesticides.

Declarations of interest

None.

Appendix: The list of abbreviations

3D-QSAR	three-dimensional quantitative structure-activity relationship
2D-QSAR	two-dimensional quantitative structure-activity relationship
CoMSIA	comparative molecular similarity indices analysis
lgBCF	logarithms of bioconcentration factor
AChR	acetylcholine receptor
NCBI	National Center for Biotechnology Information
pLC$_{50}$	negative logarithm of half maximal effective concentration
q^2	cross-validated value
n	optimal number of components
r^2	coefficient of determination
F	Fisher's test value
SEE	standard error of estimate
Q^2	perturbation prediction
dq^2/dr^2yy	slope of Q^2 with respect to correlation of the original dependent variables against the perturbed dependent variables
SEP	standard error of prediction
Q^2_{ext}	explained variance in prediction
SDEP	the calculated cross-validated standard error of prediction
TE	total energy
$\triangle E$	HOMO−LUMO energy difference
q^+	most positive Millikan charge
q^-	most negative Millikan charge
DP	dipole moment
ΔG (production)	Gibbs free energy for new compounds
ΔG (reactant)	Gibbs free energy for the target compound
TS	transition state
ΔE	reaction energy barrier

Appendix A. Supplementary data

Supplementary data to this article can be found online at https://doi.org/10.1016/j.jclepro.2019.02.156.

References

Adnane, A., Adib, G., Mounir, G., Samir, C., M'barek, C., Abdelouahid, S., Mohammed, B., Tahar, L., 2017. Combined 3D-QSAR and molecular docking study on 7, 8-dialkyl-1, 3-diaminopyrrolo-[3, 2-f] Quinazoline series compounds to understand the binding mechanism of DHFR inhibitors. J. Mol. Struct. 1139, 319–327. https://doi.org/10.1016/j.molstruc.2017.03.039.

Arnold, K., Bordoli, L., Kopp, J., Schwede, T., 2006. The SWISS-MODEL workspace: a web-based environment for protein structure homology modelling. Bioinformatics 22 (2), 195–201. https://doi.org/10.1093/bioinformatics/bti770.

Belzunces, L.P., Tchamitchian, S., Brunet, J.L., 2012. Neural effects of insecticides in the honey bee. Apidologie 43 (3), 348–370. https://doi.org/10.1007/s13592-

012-0134-0.

Cai, Q.Y., Mo, C.H., Wu, Q.T., Katsoyiannis, A., Zeng, Q.Y., 2012. The status of soil contamination by semivolatile organic chemicals (SVOCs) in China: a review. Sci. Total Environ. 389 (2), 209–224. https://doi.org/10.1016/j.scitotenv.2007.08.026.

Chen, Y., Cai, X., Jiang, L., Li, Y., 2016. Prediction of octanol-air partition coefficients for polychlorinated biphenyls (PCBs) using 3D-QSAR models. Ecotoxicol. Environ. Saf. 124, 202–212. https://doi.org/10.1016/j.ecoenv.2015.10.024.

Dil, E.A., Asfaram, A., Ghaedi, M., Ghezelbash, G.R., 2016. Modeling and optimization of Hg^{2+} ion biosorption by live yeast Yarrowia lipolytica 70562 from aqueous solutions under artificial neural network-genetic algorithm and response surface methodology: kinetic and equilibrium study. RSC Adv. 6 (59), 54149–54161. https://doi.org/10.1039/C6RA11292G.

Dil, E.A., Ghaedi, M., Asfaram, A., Mehrabi, F., 2017a. Application of modified magnetic nanomaterial for optimization of ultrasound-enhanced removal of Pb^{2+} ions from aqueous solution under experimental design: investigation of kinetic and isotherm. Ultrason. Sonochem. 36, 409–419. https://doi.org/10.1016/j.ultsonch.2016.12.016.

Dil, E.A., Ghaedi, M., Ghezelbash, G.R., Asfaram, A., 2017b. Multi-responses optimization of simultaneous biosorption of cationic dyes by live yeast Yarrowia lipolytica 70562 from binary solution: application of first order derivative spectrophotometry. Ecotoxicol. Environ. Saf. 139, 158–164. https://doi.org/10.1016/j.ecoenv.2017.01.030.

Dil, E.A., Ghaedi, M., Asfaram, A., Bazrafshan, A.A., 2018. Ultrasound wave assisted adsorption of Congo red using gold-magnetic nanocomposite loaded on activated carbon: optimization of process parameters. Ultrason. Sonochem. 46, 99–105. https://doi.org/10.1016/j.ultsonch.2018.02.040.

Dively, G.P., Kamel, A., 2012. Insecticide residues in pollen and nectar of a cucurbit crop and their potential exposure to pollinators. J. Agric. Food Chem. 60 (18), 4449–4456. https://doi.org/10.1021/jf205393x.

European Food Safety Authority, 2013. Conclusion on the peer review of the pesticide risk assessment for bees for the active substance imidacloprid. EFSA Journal 11 (1), 3066–3124. https://doi.org/10.2903/j.efsa.2015.4211.

Goulson, D., Nicholls, E., Botías, C., Rotheray, E.L., 2015. Bee declines driven by combined stress from parasites, pesticides, and lack of flowers. Science 347 (6229), 165–174. https://doi.org/10.1126/science.1255957.

Gu, W.W., Chen, Y., Zhang, L., Li, Y., 2016. Prediction of octanol-water partition coefficient for polychlorinated naphthalenes through three-dimensional QSAR models. Hum. Ecol. Risk Assess. 23 (1), 40–55. https://doi.org/10.1080/10807039.2016.1219650.

Gu, W.W., Chen, Y., Li, Y., 2017. Attenuation of the atmospheric migration ability of polychlorinated naphthalenes (PCN-2) based on three-dimensional QSAR models with Full factor experimental design. Bull. Environ. Contam. Toxicol. 99 (2), 276–280. https://doi.org/10.1007/s00128-017-2123-5.

Hajipour, A.R., Ghorbani, S., Karimzadeh, M., Jajarmi, S., Chermahini, A.N., 2016. A DFT approach for simple and solvent assisted-proton movement: biurea as a case of study. Comput. Theor. Chem. 1084, 67–74. https://doi.org/10.1016/j.comptc.2016.03.009.

Henry, M.I., Beguin, M., Requier, F., Rollin, O., Odoux, J.F., Aupinel, P., Aptel, J.,

Tchamitchian, S., Decourtye, A., 2012. A common pesticide decreases foraging success and survival in honey bees. Science 336 (6079), 348–350. https://doi.org/10.1126/science.1215039.

Mullin, C.A., Maryann, F., Frazier, J.L., Ashcraft, S., Simonds, R., Vanengelsdorp, D., Pettis, J.S., 2010. High levels of miticides and agrochemicals in north American apiaries: implications for honey bee health. PLoS One 5 (3) e9754. https://doi.org/10.1371/journal.pone.0009754.

Reihaneh, S.S., Jahan, G., 2013. Quasi 4D-QSAR and 3D-QSAR study of the pan class I phosphoinositide-3-kinase (PI3K) inhibitors. Med. Chem. Res. 22 (4), 1587–1596. https://doi.org/10.1007/s00044-012-0151-6.

Salahinejad, M., Ghasemi, Jahan, 2013. 3D-QSAR studies on the toxicity of substituted benzenes to Tetrahymena pyriformis: CoMFA, CoMSIA and VolSurf approaches. Ecotoxicol. Environ. Saf. 105, 128–134. https://doi.org/10.1016/j.ecoenv.2013.11.019.

Tan, K., Chen, W., Dong, S., Liu, X., Wang, Y., Nieh, J.C., 2014. Imidacloprid alters foraging and decreases bee avoidance of predators. PLoS One 9 (7) e102725. https://doi.org/10.1371/journal.pone.0102725.

Tapparo, A., Giorio, C., Marzaro, M., Marton, D., Soldà, L., Girolami, V., 2011. Rapid analysis of neonicotinoid insecticides in guttation drops of corn seedlings obtained from coated seeds. J. Environ. Monit. 13 (6), 1564–1568. https://doi.org/10.1039/c1em10085h.

Tong, L.D., Guo, L.X., Lv, X.J., Li, Y., 2016. Modification of polychlorinated phenols and evaluation of their toxicity, biodegradation and bioconcentration using three-dimensional quantitative structure-activity relationship models. J. Mol. Graph. Model. 71, 1–12. https://doi.org/10.1016/j.jmgm.2016.10.012.

Tush, G.M., Anstead, M.I., 1997. Pralidoxime continuous infusion in the treatment of organophosphate poisoning. Ann. Pharmacother. 31 (4), 441–444. https://doi.org/10.1046/j.1365-2036.1997.147323000.x.

Wang, X.L., Chu, Z.H., Yang, J.W., 2017a. Pentachlorophenol molecule design with lower bioconcentration through 3D-QSAR associated with molecule docking. Environ. Sci. Pollut. Res. 24 (32), 25114–25125. https://doi.org/10.1007/s11356-017-0129-5.

Wang, X.L., Gu, W.W., Guo, E.M., Cui, C.Y., Li, Y., 2017b. Assessment of long-range transport potential of polychlorinated Naphthalenes based on three-dimensional QSAR models. Environ. Sci. Pollut. Res. 24 (17), 14802–14818. https://doi.org/10.1007/s11356-017-8967-8.

Wang, M., Tian, Y., Du, Y.Y., Sun, G.B., Xu, X.D., Jiang, H., Xu, H.B., Meng, X.B., Zhang, J.Y., Ding, S.L., Zhang, M.D., Yang, M.H., Sun, X.B., 2017c. Protective effects of Araloside C against myocardial ischaemia/reperfusion injury: potential involvement of heat shock protein 90. J. Cell Mol. Med. 21 (9), 1870–1880. https://doi.org/10.1111/jcmm.13107.

Williamson, S.M., Willis, S.J., Wright, G.A., 2014. Exposure to neonicotinoids influences the motor function of adult worker honeybees. Ecotoxicology 23 (8), 1409–1418. https://doi.org/10.1007/s10646-014-1283-x.

Yang, E.C., Chang, H.C., Wu, W.Y., Chen, Y.W., 2012. Impaired olfactory associative behavior of honeybee workers due to contamination of imidacloprid in the larval stage. PLoS One 7 (11), e49472. https://doi.org/10.1371/journal.pone.0049472.